



## Direct Identification of Dilute Surface Spins on Al<sub>2</sub>O<sub>3</sub>: Origin of Flux Noise in Quantum Circuits

S. E. de Graaf,<sup>1,\*</sup> A. A. Adamyan,<sup>2</sup> T. Lindström,<sup>1</sup> D. Erts,<sup>3</sup> S. E. Kubatkin,<sup>2</sup>  
A. Ya. Tzalenchuk,<sup>1,4</sup> and A. V. Danilov<sup>2</sup>

<sup>1</sup>National Physical Laboratory, Hampton Road, Teddington, TW11 0LW, United Kingdom

<sup>2</sup>Department of Microtechnology and Nanoscience, Chalmers University of Technology, SE-412 96 Göteborg, Sweden

<sup>3</sup>Institute of Chemical Physics, University of Latvia, LV 1586, Latvia

<sup>4</sup>Royal Holloway, University of London, Egham, TW20 0EX, United Kingdom

(Received 20 September 2016; published 31 January 2017)

An on-chip electron spin resonance technique is applied to reveal the nature and origin of surface spins on Al<sub>2</sub>O<sub>3</sub>. We measure a spin density of  $2.2 \times 10^{17}$  spins/m<sup>2</sup>, attributed to physisorbed atomic hydrogen and  $S = 1/2$  electron spin states on the surface. This is direct evidence for the nature of spins responsible for flux noise in quantum circuits, which has been an issue of interest for several decades. Our findings open up a new approach to the identification and controlled reduction of paramagnetic sources of noise and decoherence in superconducting quantum devices.

DOI: 10.1103/PhysRevLett.118.057703

It is universally accepted that noise and decoherence affecting the performance of superconducting quantum circuits are consistent with the presence of spurious two-level systems (TLSs) (see [1] for a recent review). In recent years, bulk defects have been generally ruled out as the dominant source, and the search has focused on surfaces and interfaces [2–4]. Despite a wide range of theoretical models [5–13] and experimental efforts [2,14–16], the origin of these surface TLSs still remains largely unknown, making further mitigation of TLS-induced noise and decoherence extremely challenging.

Because of its many unique properties, Al<sub>2</sub>O<sub>3</sub> is important for a wide range of emerging technologies and is the mainstay of almost all solid-state quantum devices [1], e.g., as a low-loss substrate for superconducting resonators and as an amorphous oxide in Josephson junctions. Here we explicitly focus on Al<sub>2</sub>O<sub>3</sub> in the context of quantum computing technologies and the presence of unwanted material defects. A variety of models have been suggested that could explain the ubiquitous  $1/f$  noise and high level of decoherence found in solid-state quantum devices [1]. Noise in superconducting resonators and charge qubits is typically derived from a bath of electric dipoles coupling to the device, while in superconducting quantum interference devices (SQUIDs) and flux qubits a bath of magnetic dipoles results in similar  $1/f$  noise and decoherence. To explain the observed flux noise in SQUIDs it has been suggested that surface functionalization results in electron-spin exchange via hyperfine interactions [9] or a bath of paramagnetic ions [8]. Recent experiments point towards the formation of a surface spin glass and Ruderman-Kittel-Kasuya-Yoshida interactions [10,14] and spin diffusion [16,17]. Widely different types of spin defects have been suggested as possible sources of flux noise, for example,

surface dangling bonds [14,18], adsorbed molecules [8,11,19], or intrinsic nuclear spins [9], and recent results provide strong experimental evidence for paramagnetic species being responsible for flux noise [20]. Similarly, a wide range of models seek to explain the electrically coupled TLSs in resonators and charge qubits where the latest results indicate similar mechanisms at interfaces [2,3,7,13,15]. *Ab initio* studies have suggested several possible candidates for charge coupled TLS, such as hydrogen and hydroxyl defects [6] or tunneling of protons [12].

Here we use our recently developed [21] on-chip electron spin resonance (ESR) technique that allows us to detect spins with a very low surface coverage. We combine this technique with various surface treatments specifically to reveal the nature of native surface spins on Al<sub>2</sub>O<sub>3</sub>. On a large number of samples we resolve three ESR peaks with the measured total paramagnetic spin density  $n = 2.2 \times 10^{17}$  m<sup>-2</sup>, which matches the density inferred from the flux noise in SQUIDs [5,14]. We show that two of these peaks originate from physisorbed atomic hydrogen that appears on the surface as a by-product of water dissociation [22]. We suggest that the third peak is due to molecular oxygen on the Al<sub>2</sub>O<sub>3</sub> surface captured at strong Lewis base defect sites [23,24], producing charged O<sub>2</sub><sup>-</sup>.

ESR is a nondestructive technique used to probe the nature and concentration of paramagnetic centers and their interaction with the environment. In conventional ESR a sample is placed in a 3D cavity and the transitions between the spin states of the sample are detected by measuring the microwave energy absorption as a function of magnetic field. The figure of merit for conventional spectrometers is the total detectable number of spins in the sample, typically on the order of  $10^{13}$ , in a mm-sized volume. Here we

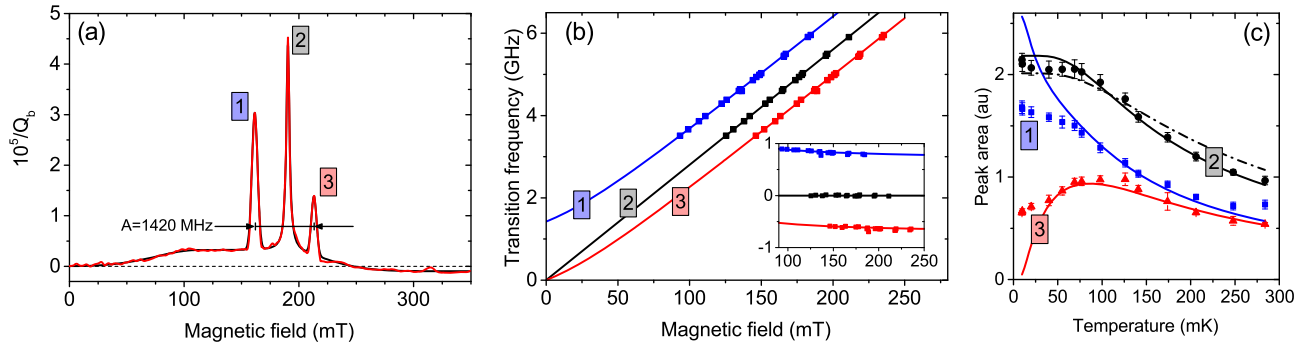


FIG. 1. Spin energy spectrum and characteristics. (a) Spectrum observed (red) at 10 mK with a fit (black). An excellent fit is obtained for a Lorentzian central peak (peak 2) and Gaussian satellite peaks (peaks 1 and 3). The broad spin background is fit to a wide Gaussian onset followed by a constant contribution to the dissipation over almost 100 mT. The shown quantity  $Q_b^{-1} = Q^{-1}(B) - Q^{-1}(B = 0)$  is the magnetic-field-associated losses, obtained from the quality factor  $Q$ . See Supplemental Material [27] for details. (b) Extracted peak positions for a large number of resonators with different frequencies jointly fitted to the energy level transitions of our model. Inset shows the same data where a constant slope of  $g = 2.0$  has been subtracted. (c) Temperature dependence of the extracted peak areas fitted to the expected temperature dependence. Solid black line is for a doublet ( $S = 1/2$ ) spin ensemble while the black dashed line corresponds to the best fit to a triplet ( $S = 1$ ). Error bars are 95% confidence bounds to spectral fits such as the fit presented in (a).

interrogate spins using an on-chip superconducting micro-resonator ESR technique [25,26] based on magnetic-field-resilient planar NbN resonators [21] fabricated on top of  $\text{Al}_2\text{O}_3$ . These on-chip spectrometers achieve better sensitivity owing to much higher quality ( $Q$ ) factors and stronger coupling to the spins. For these on-chip spectrometers the relevant figure of merit is the minimum density of spins. We can resolve about  $10^{13}$  spins per  $\text{m}^2$ . This enables us to probe the chemical nature of very dilute surface spins. Further details about the measurement method can be found in the Supplemental Material [27].

Figure 1(a) shows the central result of this Letter: the ESR signal due to paramagnetic species on the annealed surface of  $\alpha\text{-Al}_2\text{O}_3(0001)$ . The measured ESR (red) and fit (black) show a Lorentzian central peak (peak 2, with a linewidth  $\gamma_2/2\pi = 87$  MHz) accompanied by two Gaussian satellites (peaks 1 and 3, both with a linewidth of  $\Delta/2\pi = 90$  MHz) on top of a very wide spin signal “pedestal,” here with an onset at about 50 mT.

By measuring many devices and extracting the peak positions we are able to reconstruct the spin energy spectrum, shown in Fig. 1(b). The simplest interpretation of the spectrum is that of two independent spectra: an ensemble of  $S = 1/2$  electron spins coupled to  $I = 1/2$  nuclear spins [peaks 1 and 3 in Fig. 1(a)] together with a  $g = 2.0$  electron spin ensemble (peak 2), justified by the excellent fit as well as the observed temperature dependence (see below). The extracted hyperfine splitting is  $A = 1423.0 \pm 4.4$  MHz, precisely that of atomic hydrogen. Gyromagnetic ratios for both spin systems are  $g = 2.0$ , with an absolute accuracy limited by screening and flux focusing effects in the superconducting resonator. The  $g$  factors are, however, the same to within at least 0.1%. Rotating the magnetic field in the surface plane reveals unchanged spin-system parameters [27], an indication that

the spins are decoupled from the bulk  $\text{Al}_2\text{O}_3$  crystalline field; this is also supported by the unperturbed hyperfine splitting of H. Remarkably, the hydrogen is weakly physisorbed on the surface.

Further insight can be gained from the temperature dependence of the ESR transitions, shown in Fig. 1(c). We obtain an excellent fit to the expected spin polarization for our proposed spin system down to 50 mK. At zero temperature, spins will only populate the ground state of their respective spin community. The existence of two nonvanishing peaks in the spectrum down to mK temperatures thus shows that there are two independent spin communities. Furthermore, the fit allows us to attribute the central peak to a  $S = 1/2$  doublet state. Other configurations ( $S > 1/2$ ) will result in a much weaker temperature dependence [see dashed line in Fig. 1(c) for a fit to  $S = 1$ ]; this means that we can rule out, for example, triplet states in  $\text{O}_2$  [19] or atomic O [30], and the excellent fit to a Lorentzian line shape makes it unlikely that intrinsic nuclear spins, for example of Nb, N, or Al [9], are involved.

In the sample presented in Fig. 1(a) the bare substrate was annealed at  $800^\circ\text{C}$  prior to the deposition of NbN to improve the surface quality. Without this step the spectrum is significantly broader [Fig. 2(a)], and Ar ion milling, which further increases the surface roughness, results in an even broader spin resonance and an increased number of spins in both communities. It is thus clear that the spins are located on the surface of  $\text{Al}_2\text{O}_3$  and are highly sensitive to the surface quality.

From a detailed analysis of the number of spins interacting with our resonator [27] we find a spin density of  $n_H = 1.2 \pm 0.5 \times 10^{17} \text{ m}^{-2}$  of hydrogen, and  $n_e = 1.0 \pm 0.5 \times 10^{17} \text{ m}^{-2}$  of the  $g = 2$  electron spins. Remarkably, the total spin density is very close to the density thought to be responsible for flux noise in SQUIDS

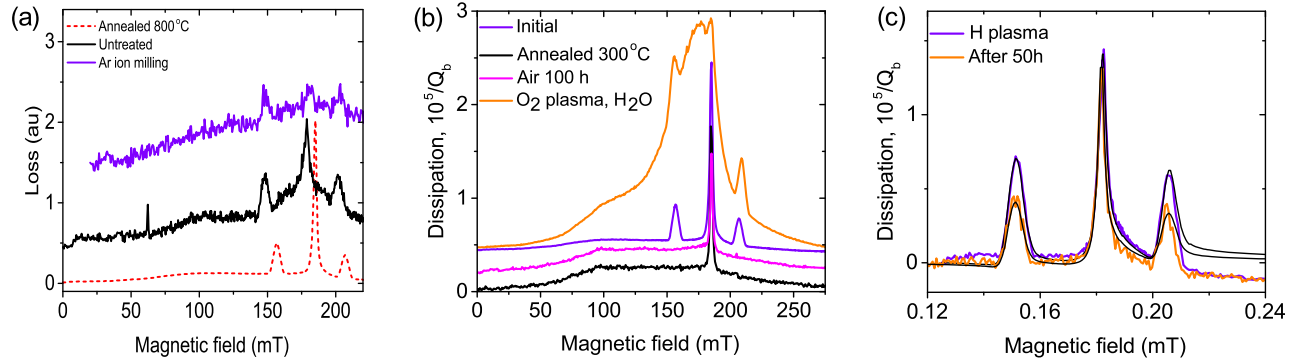


FIG. 2. Probing the surface chemistry. (a) The influence of a series of surface treatments (see text) on the measured spectrum. Curves have been offset for clarity. (b) Post fabrication annealing a sample to 300 °C removes the peaks associated with H via  $H_2$  generation. The H does not return at ambient conditions. An oxygen plasma and immersion into water returns the H peaks with the same intensity, while the central peak remains largely unaffected throughout, even in the presence of the additional broad peak after immersion in water [27]. Traces have been offset for clarity. (c) The result of exposing a sample to a H-ion plasma and subsequent relaxation back to the original spin density. The central peak is unaffected while the hydrogen spin density increased just after plasma exposure by 70%, returning to equilibrium conditions after 50 hours. Solid black lines are fits to extract spin density [27].  $T = 300$  mK.

[14,19]. The observed abundance of the two species gives a ratio  $n_H/n_e \approx 1.2$  (verified through the temperature dependence and through the collective coupling of the spins [27]).

Finally, we have explored several treatment methods in order to affect the two spin communities. Figure 2(b) shows the initial spectrum and the spectrum after annealing the same sample at 300 °C. This removes the hydrogen spins through an exothermic  $2H_{(ads)} \rightarrow H_{2(gas)}$  reaction, consistent with expected reaction barriers [8,22], and has a negligible effect on the  $g = 2$  electron spins. Long-term exposure to ambient conditions with high humidity does not affect this state. Figure 2(b) also shows the effect of exposing the sample to an oxygen plasma. After this step, exposure to water results in H peaks reappearing with the same intensity as before. The additional broad resonance has a  $g$  factor of  $2.10 \pm 0.01$ , and most likely originates from excess  $H_2O$  adsorbed on the surface [31].

Our measurements show that physisorbed atomic hydrogen is present on the surface; to understand its origin we turn to the chemistry of the alumina surface. It is well known that dissociative  $H_2O$  adsorption on pristine Al-terminated  $\alpha$ - $Al_2O_3(0001)$  leads to surface hydroxylation through an exothermic process [22,31]. The adsorbed  $H_2O$  is split into  $OH^-$  on the Al site and  $H^+$  is transferred to a nearby surface O. Hydroxylation can occur through several different reaction pathways [22,31,32]; importantly, pathways exist that lead to imperfections in the OH-terminated surface with several types of by-products, including unpaired H [22]. The perfect hydroxylated state has  $\sim 20$  OH/nm<sup>2</sup> and is expected to be ESR silent [8]. Such an OH-terminated surface has been experimentally verified using several different techniques [33,34]. Our observed surface spin density is a small fraction (1%) of the total OH density and instead links to a stable density

of physisorbed H, a by-product of the hydroxylation process. From Fig. 2(b) it is evident that moderate annealing removes these atomic H. Because no further hydroxylation can occur on the fully OH-terminated surface, no new H are generated at ambient conditions. Starting over (removing a large fraction of OH by an O plasma) and exposing the  $Al_2O_3$  surface to water results in the recovery of the same number of H.

To verify that the amount of physisorbed H reduces to a stable concentration, we exposed a sample to a H plasma [Fig. 2(c)]. This led to an increase in the ratio  $n_H/n_e = 2.0$  (without affecting the central peak), which after 50 hours exposure to atmosphere at 300 K was again reduced to  $n_H/n_e = 1.3$ , very close to the original value of 1.2. This clearly indicates that only excess physisorbed H leaves the surface and that the density is not solely governed by a thermodynamic equilibrium but by some other mechanism.

The origin of the central peak is more ambiguous, since  $g = 2.0$  is a characteristic of many different spin systems. Our findings still apply constraints on the nature of these spins. Molecular oxygen adsorbed on the Al site was suggested as a plausible candidate for flux noise [19]. While the results in Ref. [19] do suggest that neutral oxygen is involved, the signature of a triplet state would have been clearly detected in our measurements. Our observation of a doublet state instead suggests that if oxygen is present it would be in charged molecular form,  $O_2^-$  [35]. Indicatively, the observed concentration of  $g = 2$  electron spins is very close to the density of strong Lewis base sites on  $Al_2O_3$  [24]. Although the exact nature of these defectlike sites ( $D_s$ ) is still unknown, their presence is revealed by electron-donor reactions with different types of adsorbates and spin markers [23,24]. We therefore argue that  $O_2$  adsorbed via the reduction reaction  $O_2 + D_s^- \rightarrow O_2^- + D_s$  would explain the central peak. These spins are

thus always present in our experiments, since we could not avoid exposing the sample to air while mounting it in the cryostat. The homogeneously broadened central peak inferred from its Lorentzian line shape implies it is made up of a single species, and we thus note that our data alone for the central peak only indicate a single  $S = 1/2$  spin system with  $g = 2.0$  on the surface, which is a characteristic common to many different adsorbates, including  $O_2^-$ .

We find it highly intriguing that the spin densities for the two independent communities are stable at the same densities. It is possible that the concentration of H could be governed by the same  $D_s$  sites; however, any additional insight into this mechanism so far remains elusive, prompting further experimental and theoretical investigation. Finally, we also note that the broad spin signal with Gaussian onset and a flat wide plateau is present in all our experiments. The appearance of such a signal may be explained by spin-spin interactions and clustering, mechanisms that have been considered as other possible candidates for  $1/f$  flux noise [36].

Our findings provide a straightforward path towards understanding and mitigating sources of noise in superconducting quantum circuits. It has theoretically been found that hyperfine interactions provide a direct link to flux noise [9] and recent experimental results [20] show a clear peak in flux noise centered around 1.42 GHz, which is striking evidence that H produces noise even at zero applied magnetic field in superconducting qubits. Furthermore, these results shed light on previous studies showing an increase in number of TLSs after exposing dielectrics [37] and resonators [38] to H-rich conditions, and saturation of Lewis donor sites with ESR-silent molecules could explain the observed flux noise reduction in Ref. [19], which clearly provides a recipe for flux noise mitigation. The presented insight into the nature of two-level defects on  $Al_2O_3$  may lead to new processing steps that will ultimately remove these defects and increase the coherence times of quantum circuits. The reported method may also be a valuable tool to better understand the surface chemistry of  $Al_2O_3$  and other materials with implications for a wide range of applications such as catalysis, hydrogen storage, and gas sensing.

The authors would like to thank B. Brennan for carrying out SIMS analysis, S. Lara Avila for assistance with sample preparation, and V. Shumeiko, D. Golubev, J. Burnett, J. Martinis, and R. McDermott for fruitful discussions. This work was supported by the UK Government's Department for Business, Energy and Industrial Strategy, the Swedish Research Council, and the Marie Curie Initial Training Action (ITN) Q-NET.

\*sdg@npl.co.uk

[1] E. Paladino, Y. M. Galperin, G. Falci, and B. L. Altshuler, *Rev. Mod. Phys.* **86**, 361 (2014).

- [2] C. Wang, C. Axline, Y. Y. Gao, T. Brecht, Y. Chu, L. Frunzio, M. H. Devoret, and R. J. Schoelkopf, *Appl. Phys. Lett.* **107**, 162601 (2015).
- [3] J. Gao, M. Daal, A. Vayonakis, S. Kumar, J. Zmuidzinas, B. Sadoulet, B. A. Mazin, P. K. Day, and H. G. Leduc, *Appl. Phys. Lett.* **92**, 152505 (2008).
- [4] P. Macha, S. H. W. van der Ploeg, G. Oelsner, E. Il'ichev, H.-G. Meyer, S. Wünsch, and M. Siegel, *Appl. Phys. Lett.* **96**, 062503 (2010).
- [5] R. H. Koch, D. P. DiVincenzo, and J. Clarke, *Phys. Rev. Lett.* **98**, 267003 (2007).
- [6] A. M. Holder, K. D. Osborn, C. J. Lobb, and C. B. Musgrave, *Phys. Rev. Lett.* **111**, 065901 (2013).
- [7] L. Faoro and L. B. Ioffe, *Phys. Rev. B* **91**, 014201 (2015).
- [8] D. Lee, J. L. DuBois, and V. Lordi, *Phys. Rev. Lett.* **112**, 017001 (2014).
- [9] J. Wu and C. C. Yu, *Phys. Rev. Lett.* **108**, 247001 (2012).
- [10] L. Faoro and L. B. Ioffe, *Phys. Rev. Lett.* **100**, 227005 (2008).
- [11] H. Wang, C. Shi, J. Hu, S. Han, C. C. Yu, and R. Q. Wu, *Phys. Rev. Lett.* **115**, 077002 (2015).
- [12] L. Gordon, H. Aby-Farsakh, A. Janotti, and C. G. Van de Walle, *Sci. Rep.* **4**, 7590 (2014).
- [13] L. Faoro and L. B. Ioffe, *Phys. Rev. Lett.* **109**, 157005 (2012).
- [14] S. Sendelbach, D. Hover, A. Kittel, M. Mück, J. M. Martinis, and R. McDermott, *Phys. Rev. Lett.* **100**, 227006 (2008).
- [15] J. Burnett *et al.*, *Nat. Commun.* **5**, 4119 (2014).
- [16] S. M. Anton *et al.*, *Phys. Rev. Lett.* **110**, 147002 (2013).
- [17] T. Lanting, M. H. Amin, A. J. Berkley, C. Rich, S.-F. Chen, S. LaForest, and R. de Sousa, *Phys. Rev. B* **89**, 014503 (2014).
- [18] R. de Sousa, *Phys. Rev. B* **76**, 245306 (2007).
- [19] P. Kumar, S. Sendelbach, M. A. Beck, J. W. Freeland, Z. Wang, H. Wang, C. C. Yu, R. Q. Wu, D. P. Pappas, and R. McDermott, *Phys. Rev. Applied* **6**, 041001 (2016).
- [20] C. M. Quintana *et al.*, preceding Letter, *Phys. Rev. Lett.* **118**, 057702 (2017).
- [21] S. E. de Graaf, D. Davidovikj, A. Adamyany, S. E. Kubatkin, and A. V. Danilov, *Appl. Phys. Lett.* **104**, 052601 (2014).
- [22] W. H. Lu and H. T. Chen, *Phys. Chem. Chem. Phys.* **17**, 6834 (2015).
- [23] A. F. Bedilo, E. I. Shuvarakova, A. A. Rybinskaya, and D. A. Medvedev, *J. Phys. Chem. C* **118**, 15779 (2014).
- [24] D. A. Medvedev, A. A. Rybinskaya, R. M. Kenzhin, A. M. Volodin, and A. F. Bedilo, *Phys. Chem. Chem. Phys.* **14**, 2587 (2012).
- [25] D. I. Schuster *et al.*, *Phys. Rev. Lett.* **105**, 140501 (2010).
- [26] Y. Kubo, F. R. Ong, P. Bertet, D. Vion, V. Jacques, D. Zheng, A. Dréau, J.-F. Roch, A. Auffèves, F. Jelezko, J. Wrachtrup, M. F. Barthe, P. Bergonzo, and D. Esteve, *Phys. Rev. Lett.* **105**, 140502 (2010).
- [27] See Supplemental Material at <http://link.aps.org/supplemental/10.1103/PhysRevLett.118.057703>, which includes Refs. [28,29], for additional measurement details.
- [28] I. Diniz, S. Portolan, R. Ferreira, J. M. Gérard, P. Bertet, and A. Auffèves, *Phys. Rev. A* **84**, 063810 (2011).
- [29] D. A. Haas, C. Mailer, and B. H. Robinson, *Biophys. J.* **64**, 594 (1993).

- [30] J. S. M. Harvey, *Proc. R. Soc. A* **285**, 581 (1965).
- [31] K. C. Hass, W. F. Schneider, A. Curioni, and W. Andreoni, *Science* **282**, 265 (1998).
- [32] S.-Y. Ma, L.-M. Liu, and S.-Q. Wang, *J. Phys. Chem. C* **120**, 5398 (2016).
- [33] J. Sung, L. Zhang, C. Tian, G. A. Waychunas, and Y. R. Shen, *J. Am. Chem. Soc.* **133**, 3846 (2011).
- [34] P. J. Eng *et al.*, *Science* **288**, 1029 (2000).
- [35] D. B. Losee, *J. Catal.* **50**, 545 (1977).
- [36] J. Atalaya, J. Clarke, G. Schön, and A. Shnirman, *Phys. Rev. B* **90**, 014206 (2014).
- [37] J. R. Jameson, D. Ngo, C. Benko, J. P. McVittie, Y. Nishi, and B. A. Young, *J. Non-Cryst. Solids* **357**, 2148 (2011).
- [38] M. S. Khalil *et al.*, *Appl. Phys. Lett.* **103**, 162601 (2013).